https://dx.doi.org/10.4314/ijs.v24i3.4

MODELLING OF A SMALL SCALE PALM FRUIT BIOMASS-FIRED BOILER

Salako, Y. A.[1,*], Olaoye, I. O.[2], Jagun, Z. O. O.[3], Osunleke, A. S.[4] and Owolarafe, O. K.[5]

[1]Department of Agricultural Science Education, Lagos State University of Education, Oto-Ijanikin, Lagos State, Nigeria.

[2]Department of Mechanical and Agricultural Engineering, First Technical University, Ibadan, Oyo State, Nigeria.

[3]Department of Computer Engineering, Olabisi Onabanjo University, Ago-Iwoye, Ogun State, Nigeria.

[4]Department of Chemical Engineering, Obafemi Awolowo University, Ile-Ife, Osun State, Nigeria.

[5]Department of Agricultural and Environmental Engineering, Obafemi Awolowo University, Ile-Ife, Osun State, Nigeria.

*__Corresponding Author's Email:__ salakoyusuf@gmail.com

(Received: 7th October, 2022; Accepted: 19th December, 2022)

ABSTRACT

This study developed a mathematical model for the operation of a small scale palm fruit biomass-fired autoclave boiler and validated the model developed. These were with a view to providing an insight into the theoretical prediction of the boiler performance under different operating conditions and to also serve as reference point for scaling up. Models were developed using fundamental equations that apply conservation laws and were validated by comparing predicted results from theoretical combinations of the operating conditions with the experimental results obtained. The amount of air required per kg of shell, fiber and EFB as calculated were 6.66, 5.98 and 6.27 kg, respectively. Therefore, 20% of the optimum air required were introduced for all fuel combinations as excess air in order to achieve a better combustion process. Some of the values for predicted / experimental results for steam temperature profile include: 154 / 156 °C; 158 / 150 °C; 166 / 159 °C; 149/ 161 °C after 60 minutes firing time while some of the predicted / experimental results for furnace core temperature profile after 60 minutes firing time include: 704 / 605 °C; 678 / 611°C; 595 / 613 °C; 650 / 640 °C; 637 / 640 °C etc. The predicted result obtained were in line with the experimental result as the result of the model validation showed that the predicted and experimental values of average steam temperature and furnace core temperature compared well with overall deviation value of about 0.12 and 1.68%.

Keywords: Modelling, Palm fruit, Biomass-fired, Boiler; Model validation, Scale-up.

INTRODUCTION

Steam boilers today range in size from those required to heat a small-size home to the very large ones used in large scale processing industries. The fundamental requirement for a boiler system production of smooth and continuous energy flow. To satisfy this requirement, it is desirable that the rate and quantity of steam generation be properly controlled so that the production and consumption of steam energy can be maintained in equilibrum at all times (Mahlia *et al.*, 2003). This can only be achieved through proper understanding of theory of the boiler operation. Modelling provides key information as to the characteristics that are vital for the investigation and prediction of the boiler's performance. It also helps in measuring the performance of existing or proposed systems under different operating schemes (Mahlia *et al.*, 2003).

A number of transient heat exchanger models with a wide range of complexity have been developed since the1970's, and most of them came with a system model. Most recent attempts divided the heat exchanger into thermal segments to find overall performance (Xuan *et al.*, 2006). Generally, boiler models can either be derived from fundamental laws of physics or based on measured data from real plant operation. The first approach considers mass, momentum, and energy conservation as well as the laws of heat and mass transfer. The second approach utilizes system identification techniques to develop black-box models that describe the system in a particular operating_condition. Boiler modelling using the first approach can be found in the work of Mahlia *et al.* (2003); Haq *et al.* (2016) and Tawfeic *et al.* (2013) among others.

A working example of the second approach can be found in Nazaruddin *et al.* (2008a; 2008b). Other methods include: model based control system, distributed parameter methods, slip-flow model, finite volume method, moving boundary approaches, simple mathematical model describing the thermodynamic processes taking place in the system, fuzzy modeling approach (as described by Jamshidi *et al.*, 2012),

dynamic modelling based on real parameters of heat exchanger, among others. Most of these available models were on large scale boilers found in large industries. However, there is need to adapt these modelling approaches to small scale boilers to optimise boiler operations.

A lot of authors have been dealing with improving extraction efficiency and production quality of small scale palm oil production through development and performance optimization of small scale biomass fuelled boiler. Notably among the contribution of authors in the past is the characterization of the palm fruit biomass as fuel, development of adaptable small scale boiler with special focus on cost estimation, ecology point of view to reduce pollutant emission using low cost sensor to sense the trend of carbon monoxide emission (Mižáková *et al.,* 2021; Oladosu *et al.,* 2018 and Salako *et al.,* 2014). Similarly, models have also been developed to predict with accuracy the quasi-steady behavior of Organic Rankine Cycle (ORC) in order to understand some physical phenomena affecting the performance of small scale boiler. Also, simulation of small scale fixed-bed biomass thermal conversion systems, computational fluid dynamics (CFD) modelling of wood in fixed bed boiler have also been undertaken by researchers in the past (Santos *et al.,* 2017, Collazo *et al.,* 2012, Bai *et al.,* 2002). However, these existing models have not addressed the existing gap between the local production and industrial scale production of palm oil in terms of oil quality and extraction efficiency.

Therefore, in order to bridge the gap and optimize the operation of the small scale boiler for palm fruit processing, suitable model that will provide key information as to the characteristics that are vital for the investigation and prediction of the boiler's performance has to be developed. It will also help in measuring the performance of existing or proposed systems under different operating conditions and provide a basis for further optimization of its design and capacity scale-up be developed; hence, this study.

Conceptual Physical Geometry and Theory of the Biomass-fired Boiler

The palm fruit biomass-fired boiler developed, following a conceptual physical geometry as shown in Figure 1 operates on a concept of heat and mass transfer. The first law of thermodynamics requires that the rate of heat transfer from the hot fluid be equal to the rate of heat transfer to the cold one as stated by Sebastian (2002) and Sebastian and Antto (2002) that is,

$$Q = m_c C_{p,c}(T_{c,out} - T_{c,in}) = m_h C_{p,h}(T_{h,in} - T_{h,out}) \quad (1)$$

Where: m_c is the mass of cold fluid (kg)
m_h is the mass of hot fluid (kg)
C_p is the specific heat capacity (J / (kg.K))
T is the temperature of fluid (K)

Suscripts:
$_c$ denotes cold fluid
$_h$ denotes hot fluid
$_{in}$ denotes fluid inflow
$_{out}$ denotes fluid outflow

In the heat exchanger analysis, the product of the *mass flow rate* and the *specific heat* of a fluid can be combined into a single quantity. This quantity is called the heat capacity rate and is defined for the cold and hot fluid streams as stated in Equations 2 and 3, respectively.

$$C_c = m_c C_{p,c} \quad (2)$$

$$C_h = m_h C_{p,h} \quad (3)$$

Therefore heat flux (Q) can be stated as

$$Q = C_c(T_{c,out} - T_{c,in}) \quad (4)$$

$$Q = C_h(T_{h,in} - T_{h,out}) \quad (5)$$

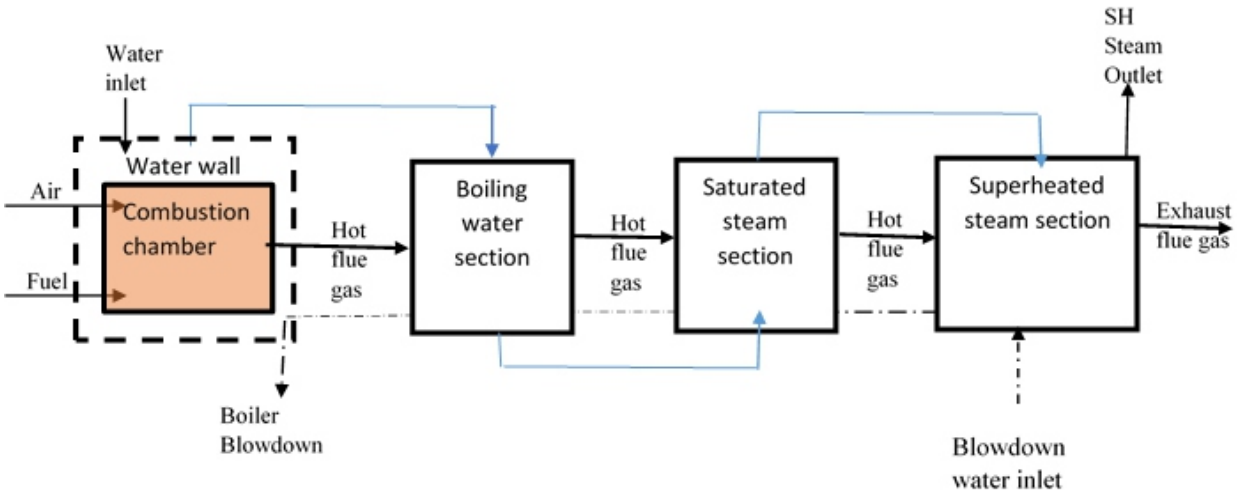

Figure 1: Conceptual physical geometry of the modified biomass fired boiler.

The fluid in the boiler which undergoes a phase-change process, has heat transfer rate

$$Q = mh_{fg} \quad (6)$$

Some fundamental physics laws were reviewed in time-dependent form, and the process model established using the following fundamental equations as stated by Jamshidi *et al.* (2012) and Mahlia *et al.* (2003).

Conservation of mass

The mass balance equation or conservation of mass is expressed by:

$$\frac{d(V\rho)}{dt} = \dot{m}_{in} - \dot{m}_{out} \quad (7)$$

Conservation of energy

The conservation of energy which is the first law of thermodynamics, can be expressed in terms of the relationship

$$\frac{d(V\rho h_{out})}{dt} = \dot{m}_{in}h_{in} - \dot{m}_{out}h_{out} + Q - W \quad (8)$$

Heat energy transfer expressions according to Mahlia *et al.* (2003) are as stated in equations 9 to 11.

Gas to metal

$$Q_g = k_g w_g^{0.6}(T_g - T_m) \quad (9)$$

Metal to fluid (one phase flow)

$$Q = kw^{0.8}(T_m - T) \quad (10)$$

Metal to fluid (two phase flow)

$$Q = k(T_m - T)^3 \quad (11)$$

Theory of heat exchange in the various sections of the boiler

Within the furnace, water flows in shells with different geometries and exchanges heat with the hot flue gas flowing through the tube arrangement. The boiler comprises of the furnace, shell and tube section. At the furnace the rate of change of heat energy at the furnace can be expressed as:

$$\frac{dQ}{dt} = Q_f + Q_a - Q_{fg} \quad (12)$$

Where: Q_f is the amount of heat energy in fuel sample (kW)

Q_a is the amount of energy in combustion air

Q_{fg} is the amount of heat energy in flue gas

As stated above, heat flux can therefore be expressed as

$$Q = m.C_p.\Delta T = \rho.V.C_p.\Delta T = h.m \quad (13)$$

Also, the amount of heat energy in fuel material is the product of its calorific (heating) value and the mass of the fuel.

That is,

$$Q_f = C_f m_f \quad (14)$$

Where: C_f is the calorific value of the fuel sample

m_f is the mass of fuel sample

C_p is the specific heat capacity

Therefore,

$$\frac{dQ}{dt} = C_f m_f + h_a m_a - h_{fg} m_{fg} \quad (15)$$

Where: h_a is the specific enthalpy of air (kJ/kg)
m_a is the mass of air (kg)
h_{fg} is the specific enthalpy of flue gas (kJ/kg)
m_{fg} is the mass of flue gas (kg)

The heat exchange between the hotter fluid in the tube and colder fluid in the shell takes place at the shell and tube section. The boiler has a fire in tube arrangement where the bulk movement of the hot flue gas from the furnace is being transferred into the tube side of the boiler. The heat energy gained is then conducted through the tube to the shell side of the boiler thereby increasing the temperature of the fluid in the shell.

The shell and tube arrangement as illustrated in Fig. 2, is the basic mode of heat exchange at various section in the boiler viz: water and steam, saturated steam and superheated steam sections. The change in heat flux in the system for both the tube and shell side are as expressed in equations 16 and 17, respectively

$$\frac{dQ_{fg}}{dt} = Q_{fg\,in} - Q_{fg\,out} - Q_{tube} - Q_{shell} \quad (16)$$

$$\frac{dQ_s}{dt} = Q_{s\,in} - Q_{s\,out} + Q_{shell} \quad (17)$$

Similarly, Equations 18 and 19 can be expressed as:

$$\frac{dQ_{fg}}{dt} = (h_{fg}.\dot{m}_{fg})_{in} - (h_{fg}\dot{m}_{fg})_{out} - q_{tube} - q_w \quad (18)$$

$$\frac{dQ_s}{dt} = (h_s.\dot{m}_s)_{in} - (h_s\dot{m}_s)_{out} + q_{shell} \quad (19)$$

Where: $Q_{fg\,in}$ energy of the flue gas flowing into the section
$Q_{fg\,out}$ energy of the flue gas flowing out of the section
Q_{tube} energy gained by the tube
Q_{shell} energy gained by the shell

Development of mathematical model for the small scale palm fruit biomass-fired boiler

Steam boiler is a complex system consisting of numerous components (as shown in Fig. 3), therefore to develop the mathematical model describing the thermodynamic processes taking place in the various components of the system, the boiler will be divided into four major subsystems and for each subsystem, mathematical models will be developed based on established modelling principles from past literatures. The subsystem models are:

i. Boiler furnace model
ii. Boiler water/steam section model
iii. Boiler saturated steam section model
iv. Boiler superheated steam section model

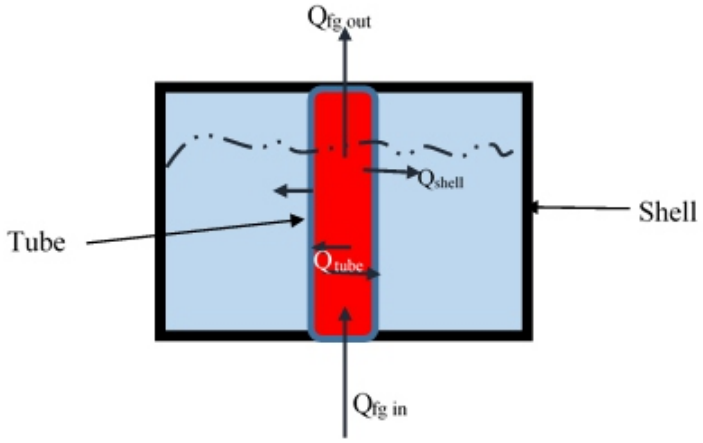

Figure 2: Rate of change of heat energy at the shell and tube section of the boiler.

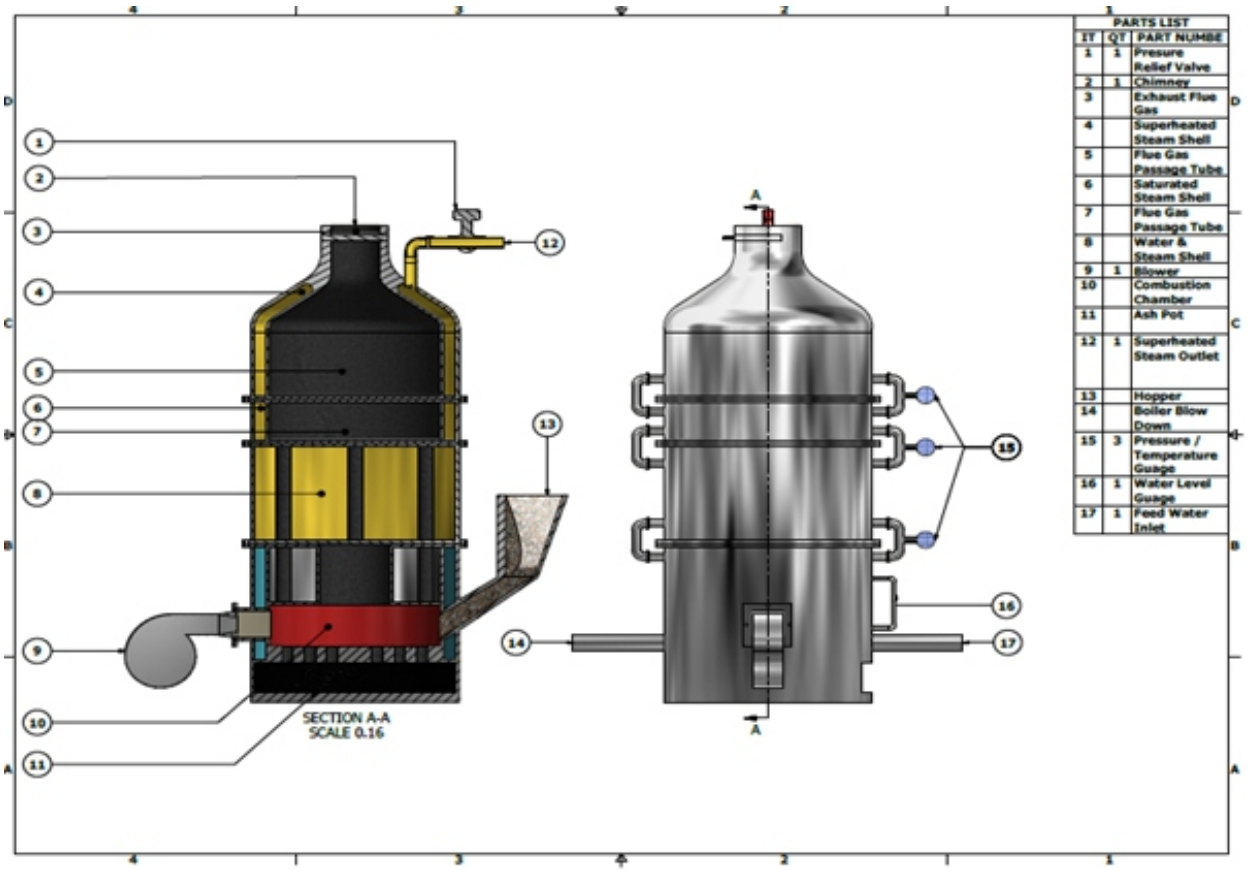

Figure 3: Detailed labelled view of the modified biomass fired boiler.

The model of the boiler is represented by a large number of differential equations following the modelling approach as expressed by Mahlia *et al.* (2003), Tawfeic (2013) and Haq *et al.* (2016) amongst others. Most of the equations are related to fluid flow, heat and mass transfer involving derivatives of time only. Simplifying assumptions have to be made to facilitate ease of solving the equations. In the analysis, the boiler is divided into sections as stated earlier and for each lumped parameter section, the steam and flue gas assumed to vary in the axial direction and linear variation with space is neglected.

3.1 General assumptions for model development and boundary conditions

Based on literatures (Mahlia *et al.*, 2003), the simplifying assumptions made are stated as follows:

i. Calorific value and moisture content of each of the fuel materials (EFB, Fiber and Shell) are assumed to be constant;
ii. Inertia of the hot gases is neglected and velocity changes take place instantaneously;
iii. Temperature of combustion gases in furnace is proportional to fuel feeding rate;
iv. Delay in heat capacitance of hot gases is neglected, i.e. temperature changes occur instantaneously in combustion gases;
v. Enthalpy of the flue gas at initial stage is taken to slightly higher than enthalpy of the ambient air;
vi. Initial ambient temperature is assumed at room temperature (36 °C);
vii. A lumped parameter approach with ordinary differential equation is used to describe the system.;
viii. No gas accummulation in the tube, i.e equal rate of flow of flue gas in and out of the tube
ix. No rate of change of stored mass in the shell and tube side; and
x. Tube wall heat resistance is neglected, i.e. tube temperature is assumed to be equal to the temperature of the hot flue gas flowing through it.

3.2 Model development

The model development involved all the different units of the boiler as detailed below, following the guidance provided by Jamshidi *et al.* (2012); Mahlia *et al.* (2003); Chin (1977) amongst others.

3.2.1 Boiler furnace modelling

Much of the behaviour of the boiler furnace (as shown in figure 4) is captured by mass and energy balances.

Mass balance:

$$\begin{bmatrix}\text{Rate of change of furnace gas flow}\end{bmatrix} = \begin{bmatrix}\text{Fuel flow rate}\end{bmatrix} + \begin{bmatrix}\text{Air flow rate}\end{bmatrix} - \begin{bmatrix}\text{Flue gas flow rate}\end{bmatrix} \quad (20)$$

The mass balance of the combustion is expressed as stated in equation 20.

Rate of change of combustion gas flow is given by Equation 21 as expressed by Mahlia *et al.*, 2003; Tawfeic, 2013 and Haq *et al.*, 2016.

$$V_{bf}.\frac{d}{dt}\rho_g = \dot{m}_f + \dot{m}_a - \dot{m}_{fg} \quad (21)$$

The energy balance for combustion chamber is given by the rate of change of energy of hot gas and is described by the differential equation.

Energy balance:

$$\begin{bmatrix}\text{Rate of change of energy of hot gas in the furnace}\end{bmatrix} = \begin{bmatrix}\text{Energy from Fuel input}\end{bmatrix} + \begin{bmatrix}\text{Energy from air input}\end{bmatrix} - \begin{bmatrix}\text{Heat energy carried by furnace gas}\end{bmatrix} \quad (22)$$

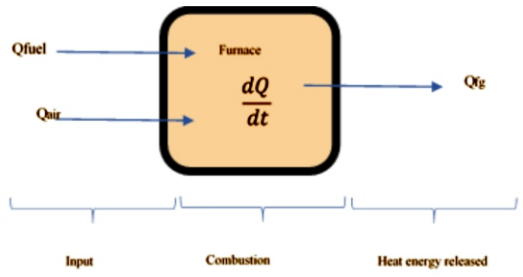

Figure 4: Rate of change of heat energy at the boiler furnace.

Therefore, the energy balance for combustion chamber is given by the rate of change of energy of hot gas and is described by the differential Equation as expressed by Mahlia *et al.* (2003) and Tawfeic (2013).

$$V_{bf}\frac{d}{dt}(\rho_g h_g) = C_f.\dot{m}_f + h_a\dot{m}_a - \dot{m}_{fg}\varepsilon(1+\frac{e_x}{100})h_{fg} \quad (23)$$

Expanding-the equation and applying necessary boundary conditions and assumptions as stated, Therefore,

$$\frac{dT_g}{dt} = \frac{1}{C_p V_{bf}\rho_{fg}}\left[C_f\dot{m}_f + h_a\dot{m}_a - \dot{m}_{fg}\varepsilon(1+\frac{e_x}{100})h_{fg}\right] \quad (24)$$

Boiler shell and tube model

The boiler consists of three shell and tube sections. These are:

i. Steam + Water section
ii. Saturated steam section
iii. Superheated steam section

Steam and Water Section

Mass balance (Shell side):

$$\begin{bmatrix}\text{Rate of change of mass of steam and water in the drum}\end{bmatrix} = \begin{bmatrix}\text{Rate of flow of feed water to the shell}\end{bmatrix} - \begin{bmatrix}\text{Rate of flow of steam out from the shell}\end{bmatrix} \quad (25)$$

$$V_w.\frac{d}{dt}\rho_w = \dot{m}_{fw} - \dot{m}_s \quad (26)$$

Energy balance (Shell side):

$$\begin{bmatrix}\text{Rate of change of energy of steam and water in the shell}\end{bmatrix} = \begin{bmatrix}\text{Energy of the feed water}\end{bmatrix} - \begin{bmatrix}\text{Energy of the steam from shell}\end{bmatrix} + \begin{bmatrix}\text{Heat energy transfered to steam} - \text{water shell}\end{bmatrix} \quad (27)$$

$$V_w \frac{d}{dt}(\rho_w h_w) = h_{fw}.\dot{m}_{fw} - h_s\dot{m}_s + q_w \quad (28)$$

Expanding the equation and applying necessary boundary conditions and assumptions as stated, Therefore

$$\frac{dT_w}{dt} = \frac{1}{C_p V_w \rho_w}\left[h_{fw}\dot{m}_{fw} - h_s\dot{m}_s + q_w\right] \quad (29)$$

Mass balance (Tube side):

$$\begin{bmatrix}\text{Rate of change of mass of flue gas in the tube}\end{bmatrix} = \begin{bmatrix}\text{Rate of flow of flue gas into the tube}\end{bmatrix} - \begin{bmatrix}\text{Rate of flow of flue gas out from the tobe}\end{bmatrix} \quad (30)$$

$$V_{fg}.\frac{d}{dt}\rho_{fg} = \dot{m}_{fg\ in} - \dot{m}_{fg\ out} \quad (31)$$

Assuming there is no gas accummulation in the tube, i.e equal rate of flow of flue gas in and out of the tube as stated earlier. Then:

$$\dot{m}_{fg\ in} = \dot{m}_{fg\ out} \quad (32)$$

Therefore, $V_{fg}.\frac{d}{dt}\rho_{fg} = 0$ (33)

Energy balance (Tube side):

$$\begin{bmatrix}\text{Rate of change of energy of flue gas in the tube}\end{bmatrix} = \begin{bmatrix}\text{Energy of the flue gas in}\end{bmatrix} - \begin{bmatrix}\text{Energy of the flue gas out from tube}\end{bmatrix} - \begin{bmatrix}\text{Heat energy gain by tube from hot flue gas}\end{bmatrix} - \begin{bmatrix}\text{Rate of energy transfer to shell from tube}\end{bmatrix} \quad (34)$$

$$V_{fg}\frac{d}{dt}(\rho_{fg}h_{fg}) = (h_{fg}.\dot{m}_{fg})_{in} - (h_{fg}\dot{m}_{fg})_{out} - q_{tube} - q_w \quad (35)$$

Expanding the equation and applying necessary boundary conditions and assumptions as stated,

$$\frac{dT_{fg}}{dt} = \frac{1}{C_p V_{fg}\rho_{fg}}\left[(h_{fg}.\dot{m}_{fg})_{in} - (h_{fg}\dot{m}_{fg})_{out} - q_{tube} - q_w\right] \quad (36)$$

Mass balance (Shell side):

$$\begin{bmatrix}\text{Rate of change of mass of steam in the shell}\end{bmatrix} = \begin{bmatrix}\text{Rate of flow of steam in to the shell}\end{bmatrix} - \begin{bmatrix}\text{Rate of flow of saturated steam out from the shell}\end{bmatrix} \quad (37)$$

$$V_{ss}.\frac{d}{dt}\rho_{ss} = \dot{m}_{s\ in} - \dot{m}_{ss\ out} \quad (38)$$

Saturated Steam Section

Energy balance (Shell side):

$$\begin{bmatrix}\text{Rate of change of energy in the saturated steam shell}\end{bmatrix} = \begin{bmatrix}\text{Energy of the steam in to the sat.steam shell}\end{bmatrix} - \begin{bmatrix}\text{Energy of sat.steam out from shell}\end{bmatrix} + \begin{bmatrix}\text{Heat energy transfered to steam from tube}\end{bmatrix} \quad (39)$$

$$V_{ss}\frac{d}{dt}(\rho_{ss}h_{ss}) = (h_s\dot{m}_s)_{in} - (h_{ss}\dot{m}_{ss})_{out} + q_{ss} \quad (40)$$

Following the modelling procedure as described in the water and steam section, the differential equation to express the temperature profile at the shell in the saturated steam section will be given as:

$$\frac{dT_{ss}}{dt} = \frac{1}{C_p V_{ss}\rho_{ss}}\left[h_s\dot{m}_s - h_{ss}\dot{m}_{ss} + q_{ss}\right] \quad (41)$$

Mass balance (Tube side):

$$\begin{bmatrix}\text{Rate of change of mass of flue gas in the sat.tube}\end{bmatrix} = \begin{bmatrix}\text{Rate of flow of flue gas in to the sat.tube}\end{bmatrix} - \begin{bmatrix}\text{Rate of flow of flue gas out from the sat.tube}\end{bmatrix} \quad (42)$$

$$V_{fg/st}\frac{d}{dt}\rho_{fg/st} = \dot{m}_{fg\ in/st} - \dot{m}_{fg\ out/st} \quad (43)$$

Assuming there is no gas accummulation in the tube, i.e equal rate of flow of flue gas in and out of the tube. Then:

$$\dot{m}_{fg\ in/st} = \dot{m}_{fg\ out/st} \quad (44)$$

Therefore, $V_{fg/st}\frac{d}{dt}\rho_{fg/st} = 0$ (45)

Energy balance (Tube side):

$$\begin{bmatrix}\text{Rate of change of energy of flue gas in the sat. tube}\end{bmatrix} = \begin{bmatrix}\text{Energy of the flue gas in to sat.tube}\end{bmatrix} - \begin{bmatrix}\text{Energy of the flue gas out from sat.tube}\end{bmatrix} - \begin{bmatrix}\text{Heat energy gain by sat.tube from hot flue gas}\end{bmatrix} - \begin{bmatrix}\text{Rate of energy transfer to shell from sat.tube}\end{bmatrix} \quad (46)$$

$$V_{fg/st}\frac{d}{dt}(\rho_{fg/st}h_{fg/st}) = (h_{fg}.\dot{m}_{fg})_{in/st} - (h_{fg}\dot{m}_{fg})_{out/st} - q_{sat.tube} - q_{ss} \quad (47)$$

Similarly, following the modelling procedure as described in the water and steam section, the diffrential equation to express the temperature profile at the tube in the saturated steam section will be given as:

$$\frac{dT_{fg/st}}{dt} = \frac{1}{C_p V_{fg}\rho_{fg}}\left[(h_{fg}.\dot{m}_{fg})_{in/st} - (h_{fg}\dot{m}_{fg})_{out/st} - q_{sat.tube} - q_{ss}\right] \quad (48)$$

Superheated (SH) Steam Section
Mass balance (Shell side):

$$\begin{bmatrix}\text{Rate of change of mass of SH steam in the shell}\end{bmatrix} = \begin{bmatrix}\text{Rate of flow of sat.steam in to the shell}\end{bmatrix} - \begin{bmatrix}\text{Rate of flow of SH steam out from the shell}\end{bmatrix} \quad (49)$$

$$V_{sh}.\frac{d}{dt}\rho_{sh} = \dot{m}_{ss\ in} - \dot{m}_{sh\ out} \quad (50)$$

Energy balance (Shell side):

$$\begin{bmatrix}\text{Rate of change of energy in the SH steam shell}\end{bmatrix} = \begin{bmatrix}\text{Energy of the sat.steam in to the shell}\end{bmatrix} - \begin{bmatrix}\text{Energy of SH steam out from shell}\end{bmatrix} + \begin{bmatrix}\text{Heat energy transfered to SH steam from tube}\end{bmatrix} \quad (51)$$

$$V_{sh}\frac{d}{dt}(\rho_{sh}h_{sh}) = (h_{ss}\dot{m}_{ss})_{in} - (h_{sh}\dot{m}_{sh})_{out} + q_{sh} \quad (52) \qquad \frac{dT_{sh}}{dt} = \frac{1}{C_p V_{sh}\rho_{sh}}\left[(h_{ss}\dot{m}_{ss})_{in} - (h_{sh}\dot{m}_{sh})_{out} + q_{sh}\right] \quad (53)$$

Mass balance (Tube side):

$$\begin{bmatrix}\text{Rate of change of mass of flue gas in the SH tube}\end{bmatrix} = \begin{bmatrix}\text{Rate of flow of flue gas in to the SH tube}\end{bmatrix} - \begin{bmatrix}\text{Rate of flow of flue gas out from the SH tube}\end{bmatrix} \quad (54)$$

$$V_{fg/sh}\frac{d}{dt}\rho_{fg/sh} = \dot{m}_{fg\ in/sh} - \dot{m}_{fg\ out/sh} \quad (55)$$

Assuming there is no gas accummulation in the tube, i.e equal rate of flow of flue gas in and out of the tube. Then:

$$\dot{m}_{fg\ in/sh} = \dot{m}_{fg\ out/sh} \quad (56) \qquad \text{Therefore, } V_{fg/sh}\frac{d}{dt}\rho_{fg/sh} = 0 \quad (57)$$

Energy balance (Tube side):

$$\begin{bmatrix}\text{Rate of change of energy of flue gas in the SH tube}\end{bmatrix} = \begin{bmatrix}\text{Energy of the flue gas in to SH tube}\end{bmatrix} - \begin{bmatrix}\text{Energy of the flue gas out from SH tube}\end{bmatrix} - \begin{bmatrix}\text{Heat energy gain by SH tube from hot flue gas}\end{bmatrix} - \begin{bmatrix}\text{Rate of energy transfer to shell from SH tube}\end{bmatrix} \quad (58)$$

$$V_{fg/sh}\frac{d}{dt}(\rho_{fg/sh}h_{fg/sh}) = (h_{fg}.\dot{m}_{fg})_{in/sh} - (h_{fg}\dot{m}_{fg})_{out/sh} - q_{SH\ tube} - q_{sh} \quad (59)$$

$$\frac{dT_{fg/sh}}{dt} = \frac{1}{(C_{p\,fg}V_{fg}\rho_{fg})_{/sh}}\left[(h_{fg}.\dot{m}_{fg})_{in/sh} - (h_{fg}\dot{m}_{fg})_{out/sh} - q_{sh\ tube} - q_{sh}\right] \quad (60)$$

Model Solution and Validation

Solution to the model equations

The differential equations developed describing the thermodynamic processes taking place in the various component of the system-were solved analytically and numerically as follows:

Solution to the boiler furnace model equations

Recall from equation 24

$$\frac{dT_g}{dt} = \frac{1}{C_p V_{bf} \rho_{fg}} \left[C_f \dot{m}_f + h_a \dot{m}_a - \dot{m}_{fg} \varepsilon \left(1 + \frac{e_x}{100}\right) h_{fg} \right] \quad (61)$$

Recall, the initial temperature of the furnace gas at t=0, is assumed to be at temperature 36 °C.

Therefore,

$$T_g = \left[\frac{C_f \dot{m}_f + h_a \dot{m}_a - \dot{m}_{fg} \varepsilon \left(1 + \frac{e_x}{100}\right) h_{fg}}{C_p V_{bf} \rho_{fg}} \right] t + 36 \quad (62)$$

Solution to the boiler (steam/water section) shell and tube model equations

Shell side:

From equation 29

$$\frac{dT_w}{dt} = \frac{1}{C_p V_w \rho_w} \left[h_{fw} \dot{m}_{fw} - h_s \dot{m}_s + q_w \right] \quad (63)$$

Recall, the initial temperature of the inlet water at t=0, is assumed to be at room temperature, i.e. 36 °C.

Therefore,

$$T_g = \left[\frac{h_{fw} \dot{m}_{fw} - h_s \dot{m}_s - q_w}{C_p V_w \rho_w} \right] t + 36 \quad (64)$$

Tube side:

From equation 36

$$\frac{dT_{fg}}{dt} = \frac{1}{C_p V_{fg} \rho_{fg}} \left[(h_{fg} . \dot{m}_{fg})_{in} - (h_{fg} \dot{m}_{fg})_{out} - q_{tube} - q_w \right] \quad (65)$$

Recall, as earlier determined under the boiler design specification, the temperature of the flue gas entering the water and steam section at t = 0 is 260 °C.

Therefore,

$$T_{fg} = \left[\frac{(h_{fg} . \dot{m}_{fg})_{in} - (h_{fg} \dot{m}_{fg})_{out} - q_{tube} - q_w}{C_p V_{fg} \rho_{fg}} \right] t + 260 \quad (66)$$

Solution to the boiler (saturated steam section) shell and tube model equations

Shell side:

From equation 41

$$\frac{dT_{ss}}{dt} = \frac{1}{C_p V_{ss} \rho_{ss}} \left[h_s \dot{m}_s - h_{ss} \dot{m}_{ss} + q_{ss} \right] \quad (67)$$

As earlier determined, at the saturated steam section of the boiler, the initial temperature of the inlet steam at t=0, was determined to be T ≥ 100 °C.

Therefore,

$$T_{ss} = \left[\frac{h_s \dot{m}_s - h_{ss} \dot{m}_{ss} + q_{ss}}{C_p V_{ss} \rho_{ss}} \right] t + 100 \quad (68)$$

Tube side:

From equation 48,

$$\frac{dT_{fg/st}}{dt} = \frac{1}{C_p V_{fg} \rho_{fg}} \left[(h_{fg} . \dot{m}_{fg})_{in/st} - (h_{fg} \dot{m}_{fg})_{out/st} - q_{sat.tube} - q_{ss} \right] \quad (69)$$

Recall, as earlier determined under the boiler design specification, the temperature of the flue gas entering the saturated steam section at t = 0 is 176.93 °C.

Therefore,

$$T_{fg/st} = \left[\frac{(h_{fg} . \dot{m}_{fg})_{in/st} - (h_{fg} \dot{m}_{fg})_{out/st} - q_{sat.tube} - q_w}{C_p V_{fg} \rho_{fg}} \right] t + 176.93 \quad (70)$$

Solution to the boiler (superheated steam section) shell and tube model equations

Shell side:

From equation 53,

$$\frac{dT_{sh}}{dt} = \frac{1}{C_p V_{sh} \rho_{sh}} \left[(h_{ss} \dot{m}_{ss})_{in} - (h_{sh} \dot{m}_{sh})_{out} + q_{sh} \right] \quad (71)$$

As earlier determined, at the superheated steam section of the boiler, the initial temperature of the inlet steam at t=0, was determined to be T ≥ 130 °C.

Therefore,

$$T_{sh} = \left[\frac{(h_{ss} \dot{m}_{ss})_{in} - (h_{sh} \dot{m}_{sh})_{out} + q_{sh}}{C_p V_{sh} \rho_{sh}} \right] t + 130 \quad (72)$$

Tube side:

From equation 60,

$$\frac{dT_{fg/sh}}{dt} = \frac{1}{(C_p V_{fg} \rho_{fg})_{/sh}} \left[(h_{fg} . \dot{m}_{fg})_{in/sh} - (h_{fg} \dot{m}_{fg})_{out/sh} - q_{sh\ tube} - q_{sh} \right] \quad (73)$$

Recall, as earlier determined under the boiler design specification, the temperature of the flue gas entering the superheated steam section at t = 0 is 142.53 °C.

$$T_{fg/st} = \left[\frac{(h_{fg} . \dot{m}_{fg})_{in/sh} - (h_{fg} \dot{m}_{fg})_{out/sh} - q_{sh\ tube} - q_{sh}}{(C_p V_{fg} \rho_{fg})_{/sh}} \right] t + 142.53 \quad (74)$$

Boiler design parameters and operating conditions
Heating values of different fuel combinations
Palm fruit biomass used as fuel to fire the boiler was combined differently to establish the best possible proportion that can produce optimum boiler performance. The calorific (heating) value (CV) of EFB, fibre and shell from oil palm biomass were 13.99, 11.2 and 14.94 $MJ.kg^{-1}$, respectively, as obtained by Salako *et al*., 2009 and Najmi *et al*., 2008.
Representing EFB with 'X', fibre with 'Y' and shell with 'Z', therefore different possible combination of 'XYZ' and the heating value of each proportion can be determined.

Stoichiometric (theoretical) air and excess air
The amount of air required per kg of shell, fiber and EFB calculated following the procedure provided by Mahlia *et al*., 2003 were 6.66, 5.98 and 6.27 kg, respectively.The optimum and excess air requirement for the fuel combinations was also calculated based on the amount of air required per fuel combination. 20% excess air were introduced for all the combinations in order to achieve a better combustion process.

Theoretical boiler fuel consumption (FC)
The boiler fuel consumption was calculated as stated by JBC (2016) using equation 75 stated earlier. Using the calorific (heating) value (CV) of shell, fibre and EFB from oil palm biomass as established by Salako *et al*., 2011 and Najmi *et al*., 2008, therefore from the different fuel combination ratio established above, the boiler fuel consumption for the various combination of biomass can be calculated using.

$$FC = SP \times \frac{h_s - h_w}{BE \times LHV} \qquad (75)$$

24
Where:
FC is the boiler fuel consumption;
SP is the steam production (kg / hour)
h_s is the specific enthalpy of steam (kJ/kg)
h_w is the enthalpy of feed water (kJ/kg)
BE is the boiler efficiency (%)
LHV is the lowest heating value (kJ/kg)

Predicted and Experimental Results

Results of Programme Runs for the Boiler Model
Model equations developed were processed using Maple Mathematical Software to predict the boiler performance viz a viz the properties of the steam that will be generated. The predicted steam temperature profile of the oil palm fruit biomass fired boiler using the model developed. The result also indicated that the properties of the steam obtained varies directly with firing time. The highest predicted steam temperature obtained was 173 °C obtained at fuel combination ratio 1:8:1, while the least predicted steam temperature of 142 °C obtained at fuel combination ratio 2:7:1. The steam pressure as shown in the figure increases gradually within 30 minutes firing and increased rapidly thereafter.

Similarly, using the model equation developed to determine the predicted furnace core temperature profile, the result indicated that the predicted core furnace temperature profile increases steadily with time. The fuel samples behaved differently in terms of the predicted furnace core temperature such that the temperature recorded ranges between 777 to 410 °C this result is in line with the findings of Najmi *et al*. (2008) and Li *et al*. (2016). The predicted result also indicated that fuel samples with higher combination of shell produces better result in terms of furnace core temperature while fuel samples with higher fiber produces the least result in terms of predicted furnace core temperature.

Experimental Results
The heating value of the various fuel composition has a direct effect on the resulting steam temperature as fuel combination with higher proportion of fibre was observed to produce the best result in terms of steam temperature as the boiling point was reached faster. Although it burns quickly in the furnace which can result to drop in the temperature if corresponding rate of fuel input into the furnace is not maintained. The highest steam temperature of 161 °C was recorded when fired with fuel combination 3:5:2, closely followed by fuel combination 2:6:2 which yielded steam temperature of 160 °C. Similarly, the least value for steam temperature of 141 °C within the experimental period was recorded at fuel combination (1:2:7) with higher proportion of shell, but burns longer in the furnace therefore the frequency of fuel input is lower compare to fiber and EFB. This result is corroborated by the

findings of Salako *et al.* (2014) and also the findings of Oladosu *et al.* (2018).

Temperature of the flue gas at all the sections increases with time due to steady in-flow of fuel material and decreases along its flow path. This shows that high gas cooling rates occurred as the combustion gases flows from the main combustion area (furnace) to the exhaust . The peak of the core temperature for all the fuel samples ranges between 602 to 738 °C. Although higher core temperature was recorded at fuel samples with higher concentration of fiber, however it was also observed that more fuel was consumed during the process as discussed earlier, this is due its lower density and physical properties. This result is in line with findings of Hani *et al.* (2020) and Najmi *et al.* (2008). The average temperature difference between the saturated tube, superheated tube and the exhaust gas at the chimney was also estimated to be about 15 °C.

Validation of this Model Using Experimental Data

Figures 5 (a to v) and 6 (a to v) show the experimental results in comparison with the predicted results obtained for the steam temperature and furnace core temperature profile, respectively. The predicted result in terms of the steam temperature correlates very well with the experimental results except with the fuel combination 2:7:1 that has the least correlation coefficient. Similarly, the predicted core temperature profile obtained also compares closely with the experimental result with the exception of fuel combinations 1:8:1, 2:7:1, 1:7:2 and 3:6:1 with relatively low correlation coefficient. The low correlation coefficient obtained was observed to occur at fuel combinations with higher percentage of fiber as stated above, this is because fiber is best utilized to support other fuel materials to enhance fast combustion (Najmi *et al.,* 2008).

Generally, the predicted results obtained are in line with the experimental results as the result of the model validation shows that the predicted and experimental values of average steam temperature and furnace core temperature compared well with overall deviation values of about 0.12 and 1.68% after adopting reasonable assumptions based on literatures. The calculation of the E-value for experimental and predicted temperature profiles is calculated as follows:

$$E\% = \frac{100}{N}\sum_{i=1}^{N}\frac{|Y_e - Y_p|}{Y_e} \qquad (76)$$

Where: Y_e = Experimental temperature profile result obtained

Y_p = Predicted temperature profile result obtained

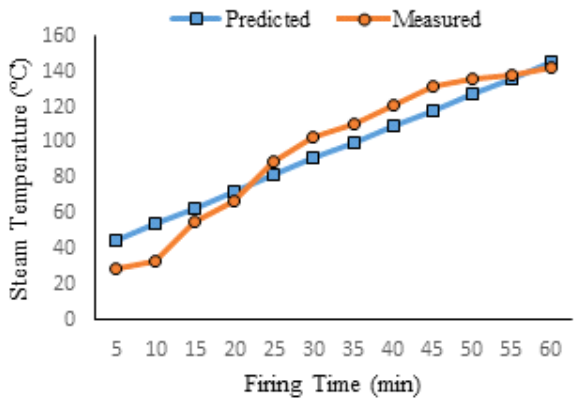

Figure 5a: Model Validation of Fuel combination 1:1:8

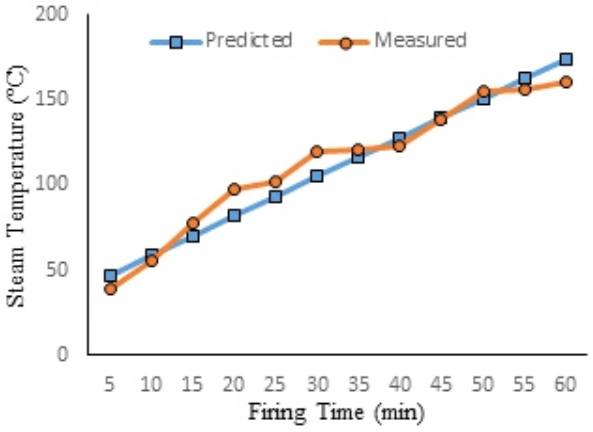

Figure 5d: Model Validation of Fuel combination 1:6:3

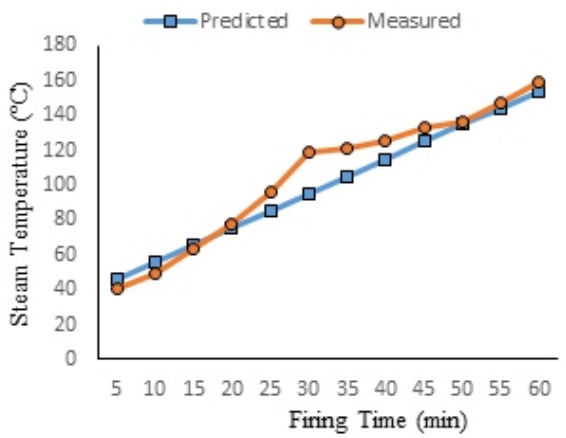

Figure 5c: Model Validation of Fuel combination 1:7:2

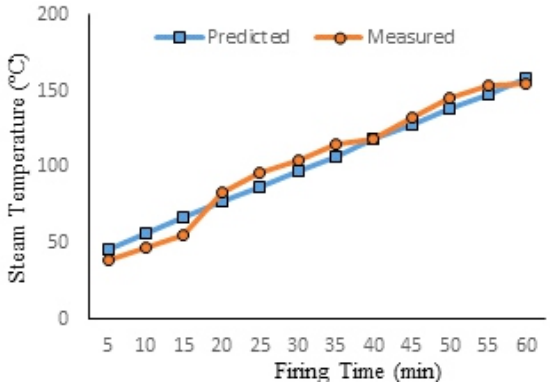

Figure 5d: Model Validation of Fuel combination 1:6:3

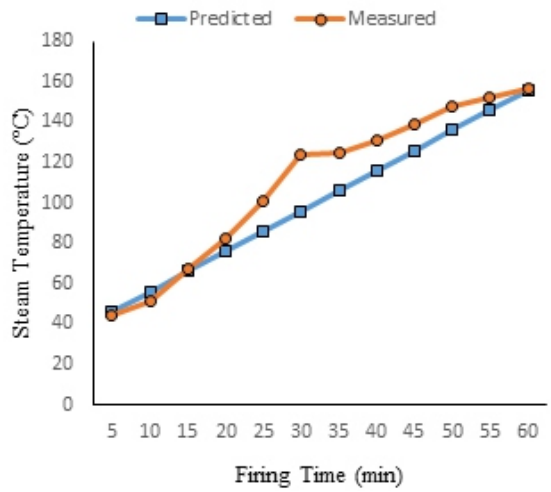

Figure 5e: Model Validation of Fuel combination 2:1:7

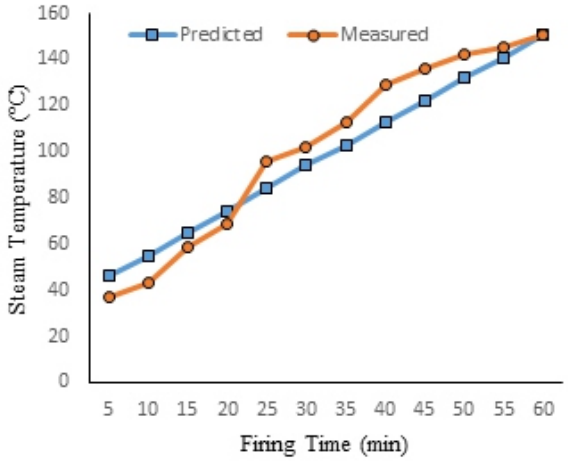

Figure 5f: Model Validation of Fuel combination 1:3:6

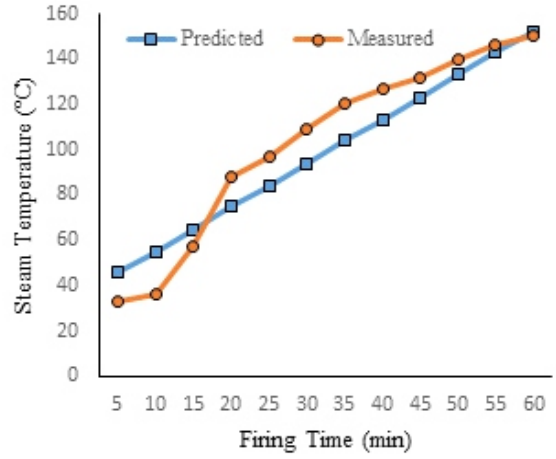

Figure 5g: Model Validation of Fuel combination 6:1:3

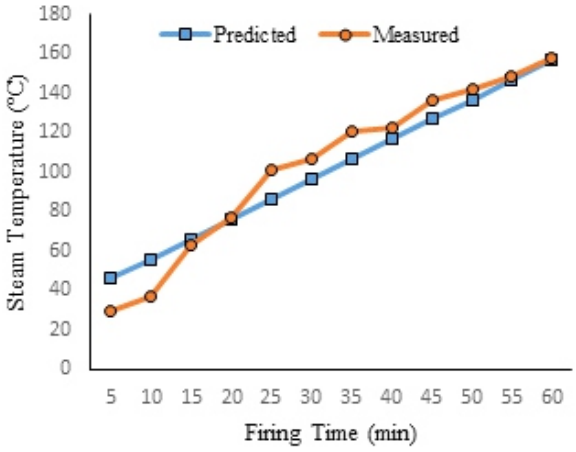

Figure 5h: Model Validation of Fuel combination 6:3:1

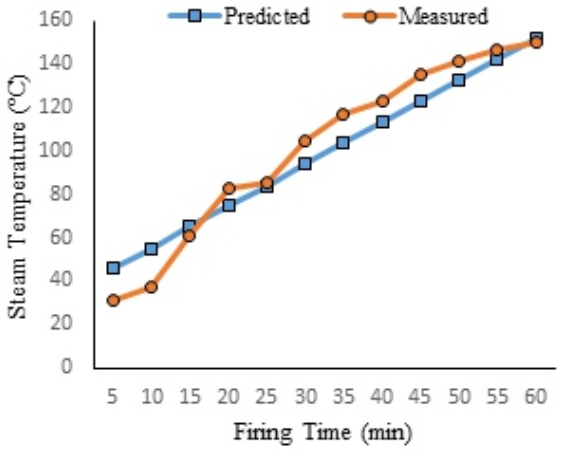

Figure 5i: Model Validation of Fuel combination 1:4:5

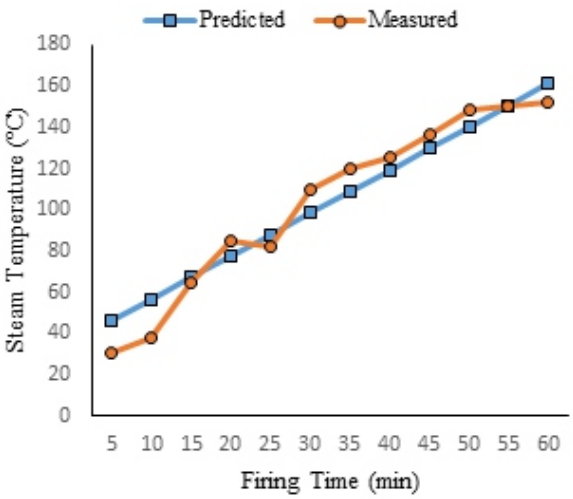

Figure 5j: Model Validation of Fuel combination 1:5:4

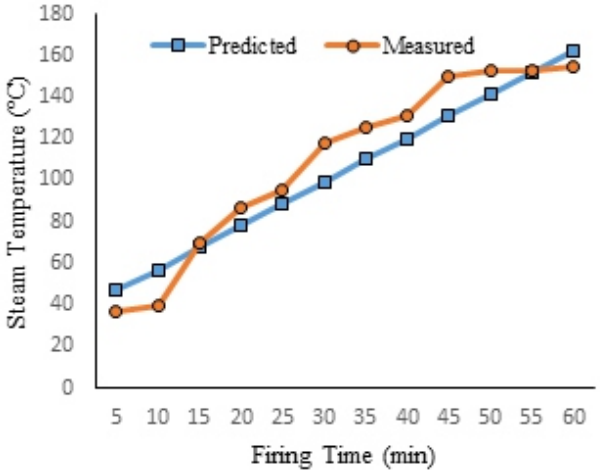

Figure 5k: Model Validation of Fuel combination 4:5:1

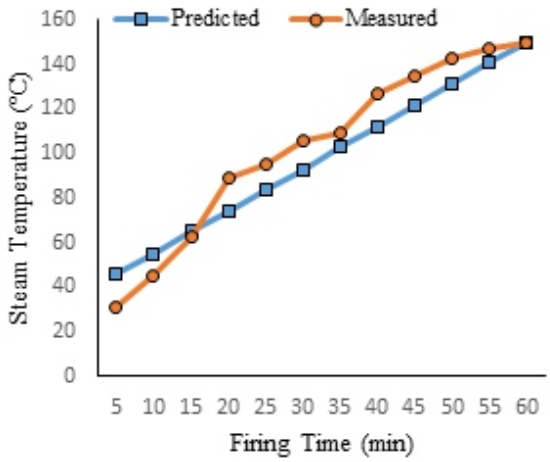

Figure 5l: Model Validation of Fuel combination 2:2:6

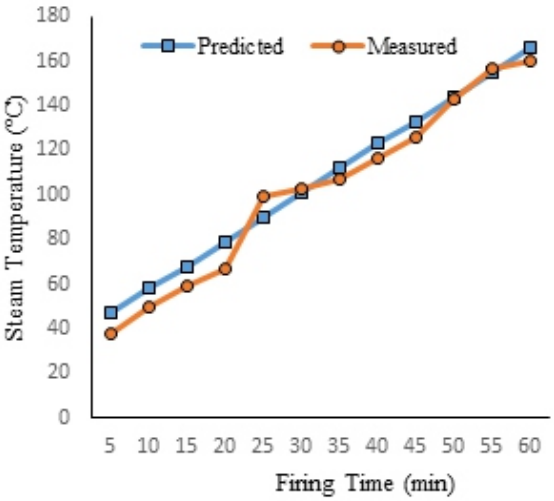

Figure 5m: Model Validation of Fuel combination 2:6:2

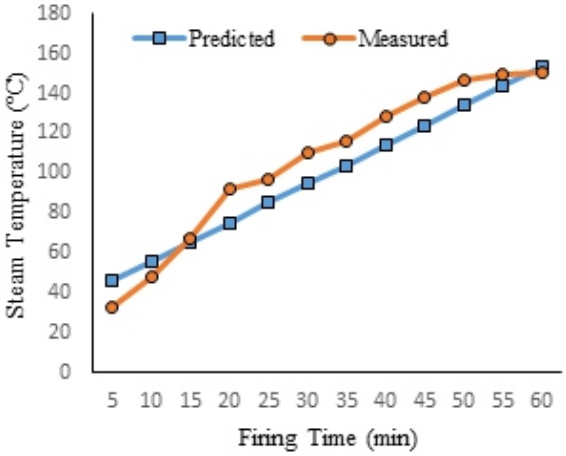

Figure 5n: Model Validation of Fuel combination 2:3:5

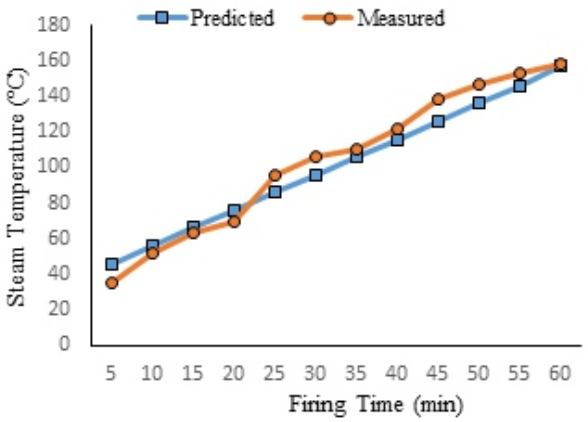

Figure 5o: Model Validation of Fuel combination 2:5:3

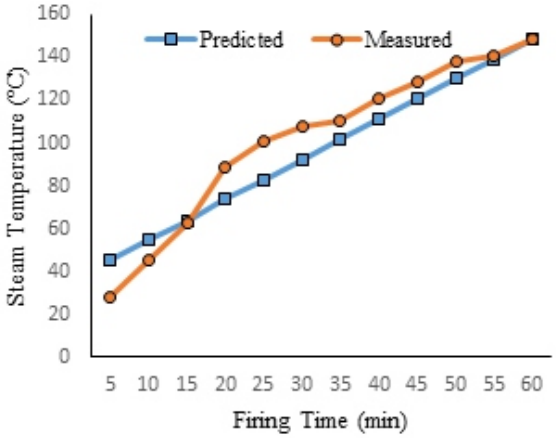

Figure 5p: Model Validation of Fuel combination 3:2:5

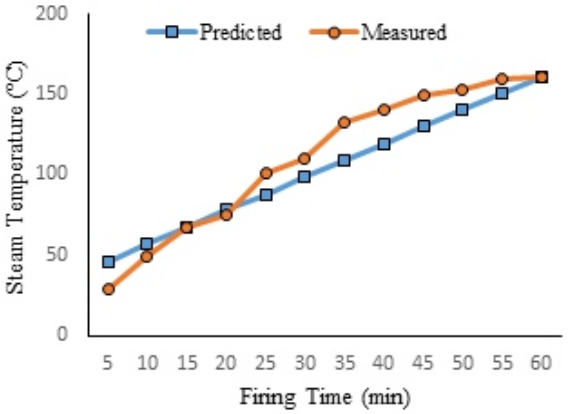

Figure 5q: Model Validation of Fuel combination 3:5:2

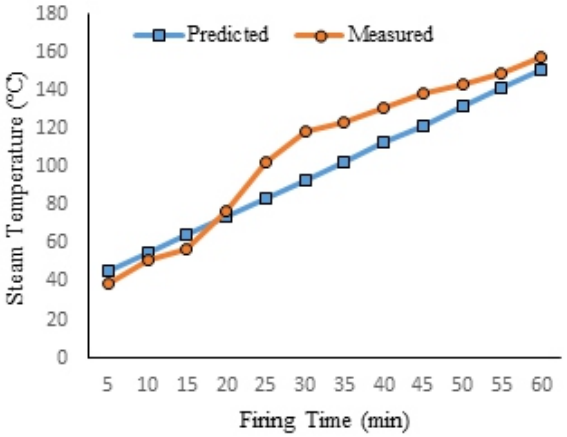

Figure 5r: Model Validation of Fuel combination 5:3:2

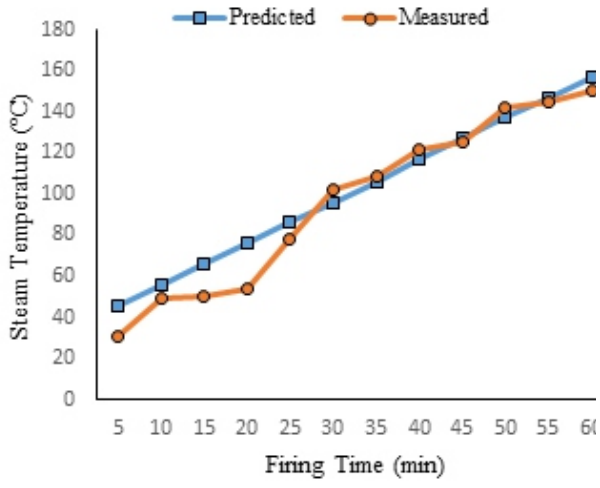

Figure 5s: Model Validation of Fuel combination 4:4:2

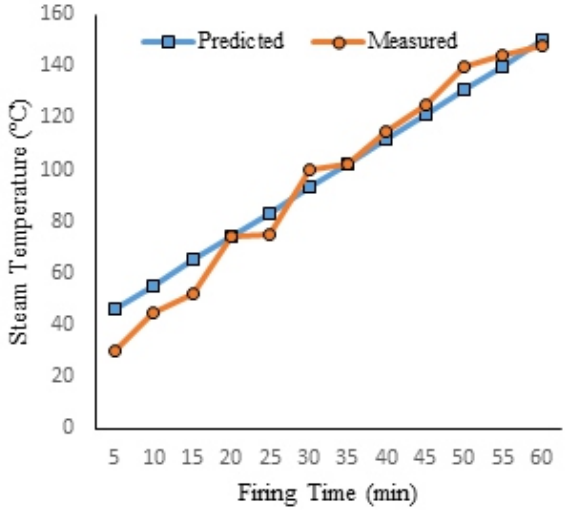

Figure 5t: Model Validation of Fuel combination 3:3:4

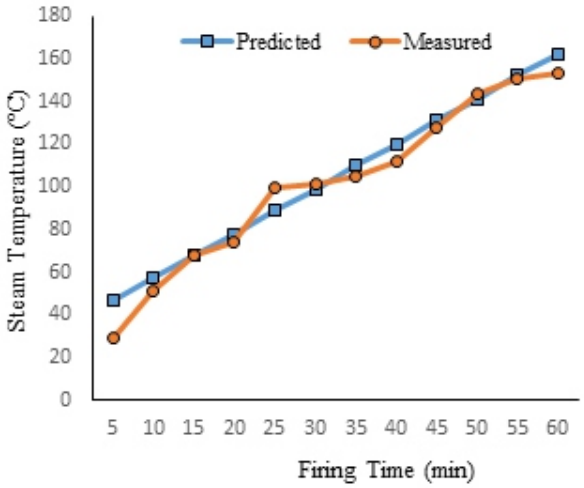

Figure 5u: Model Validation of Fuel combination 3:4:3

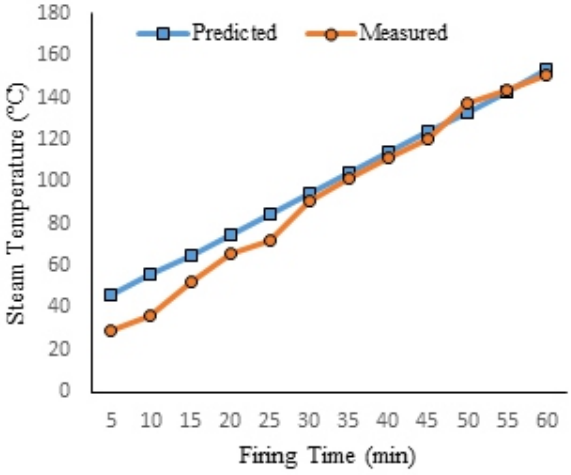

Figure 5v: Model Validation of Fuel combination 4:3:3

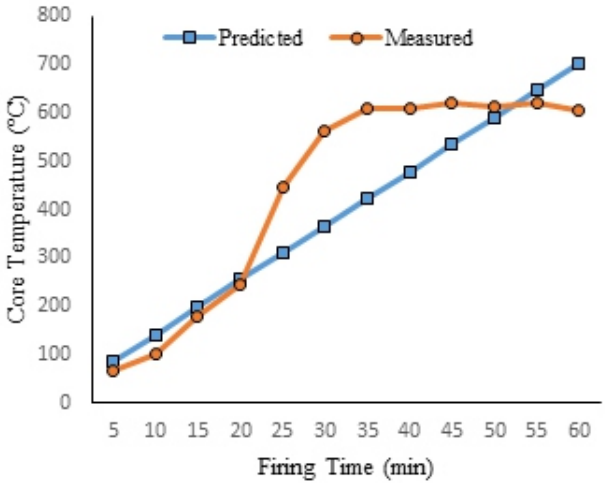

Figure 6a: Model Validation of Fuel combination 1:1:8

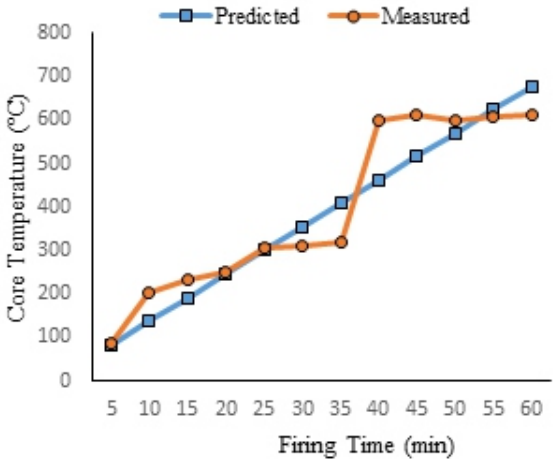

Figure 6b: Model Validation of Fuel combination 8:1:1

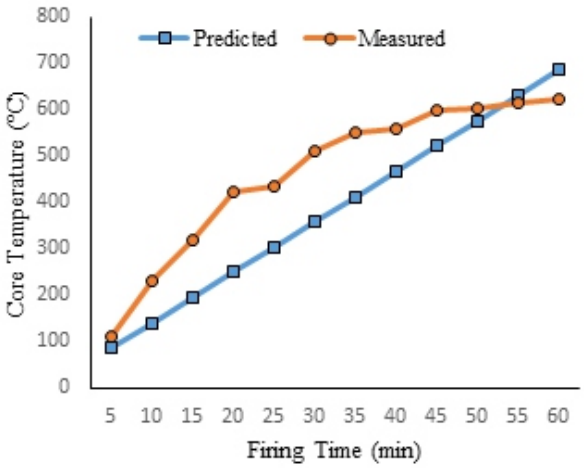

Figure 6c: Model Validation of Fuel combination 1:2:7

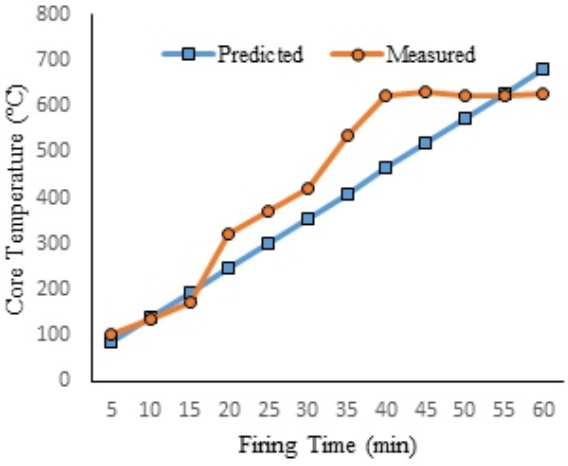

Figure 6d: Model Validation of Fuel combination 7:1:2

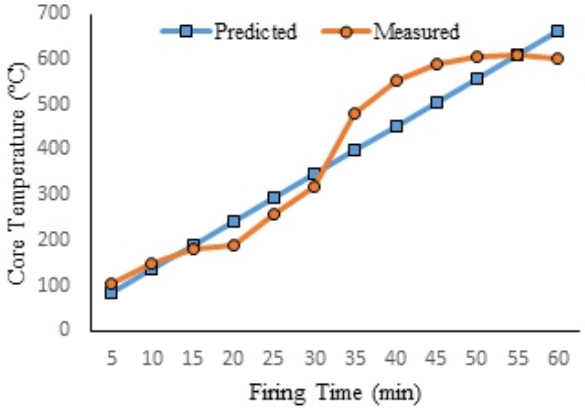

Figure 6e: Model Validation of Fuel combination 7:2:1

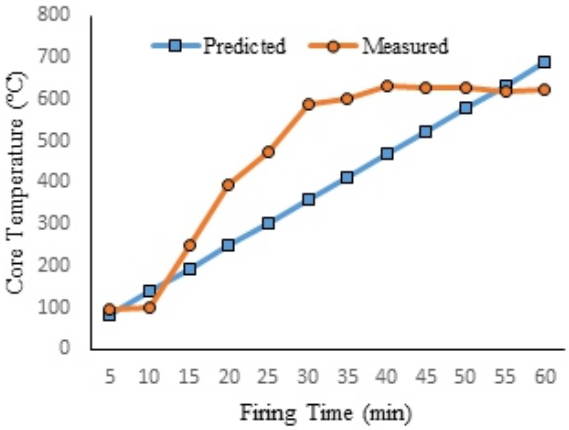

Figure 6f: Model Validation of Fuel combination 6:1:3

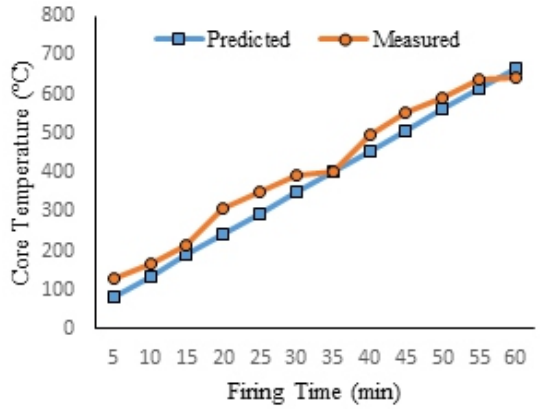

Figure 6g: Model Validation of Fuel combination 1:3:6

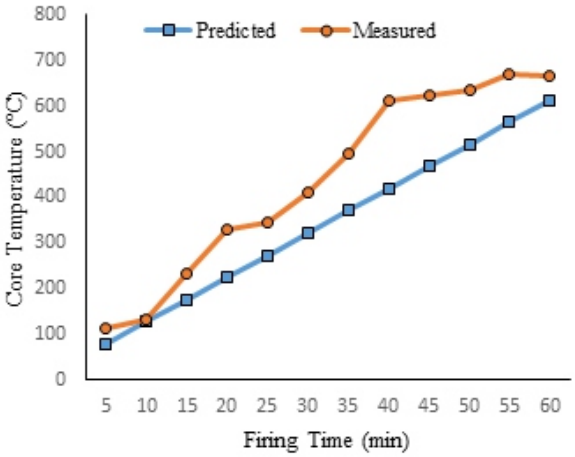

Figure 6h: Model Validation of Fuel combination 1:6:3

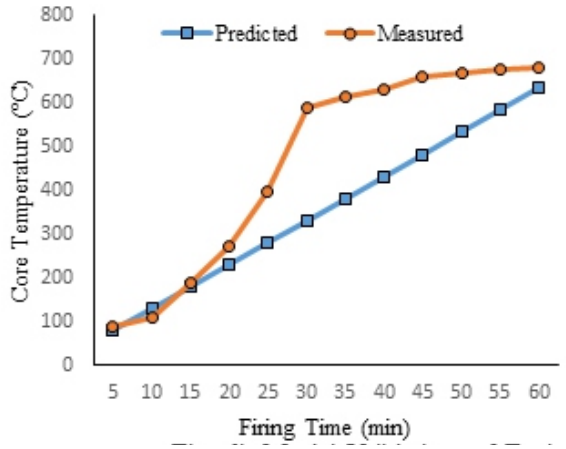

Figure 6i: Model Validation of Fuel combination 1:5:4

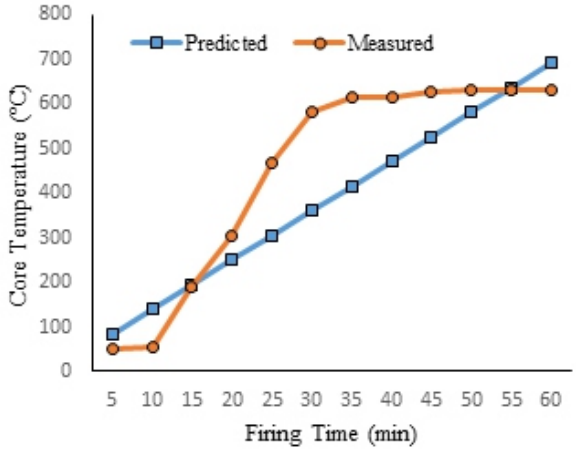

Figure 6j: Model Validation of Fuel combination 4:1:5

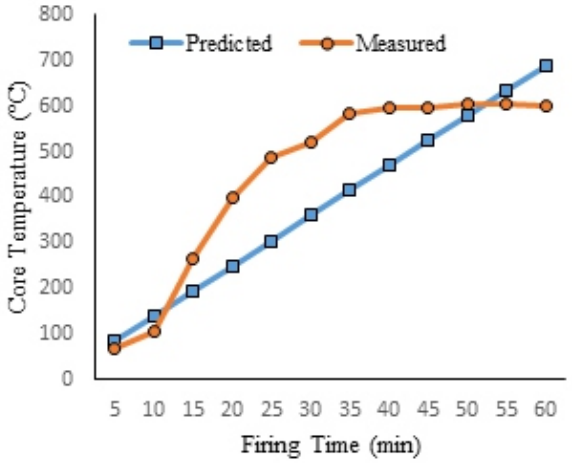

Figure 6k: Model Validation of Fuel combination 5:1:4

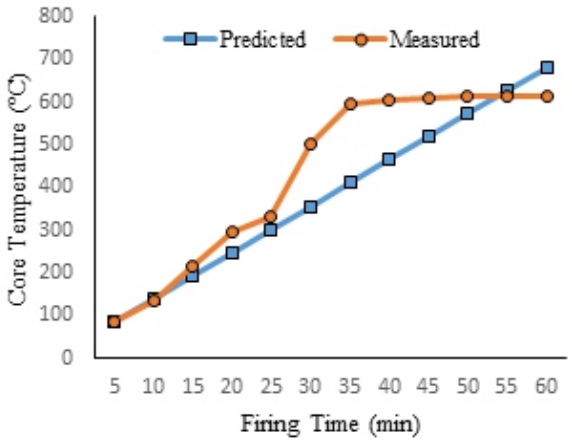

Figure 6l: Model Validation of Fuel combination 2:2:6

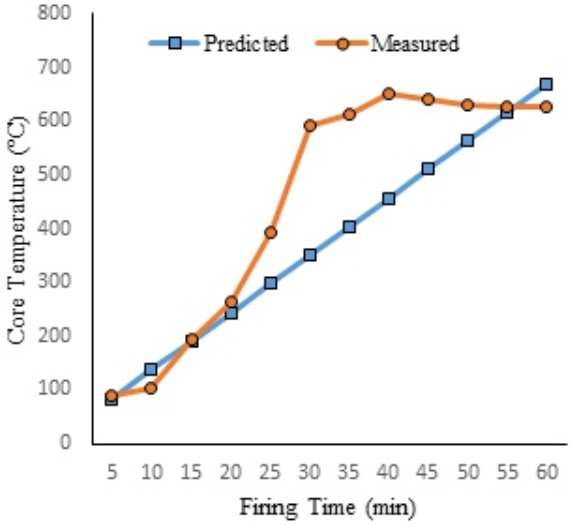

Figure 6m: Model Validation of Fuel combination 6:2:2

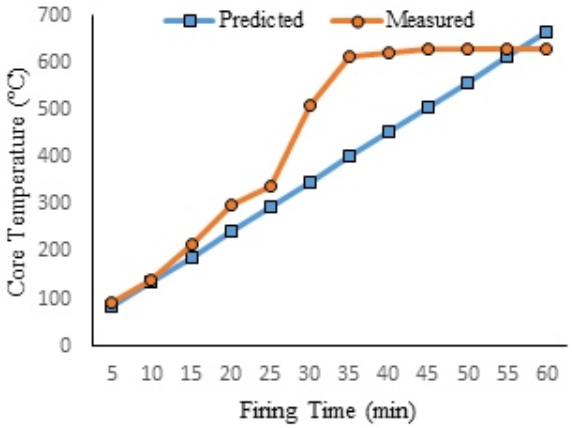

Figure 6n: Model Validation of Fuel combination 2:3:5

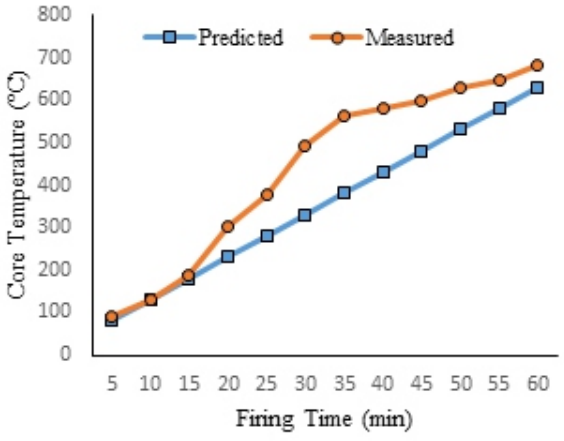

Figure 6o: Model Validation of Fuel combination 2:5:3

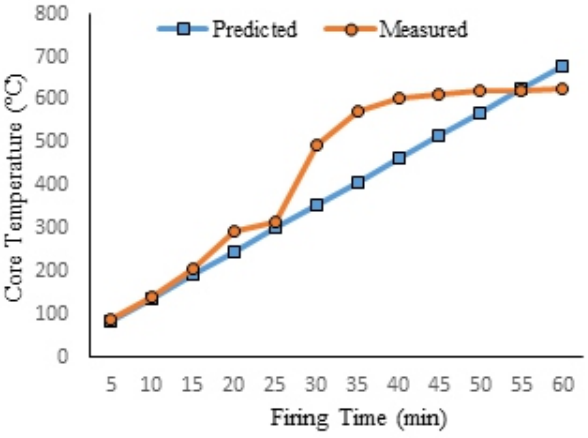

Figure 6p: Model Validation of Fuel combination 3:2:5

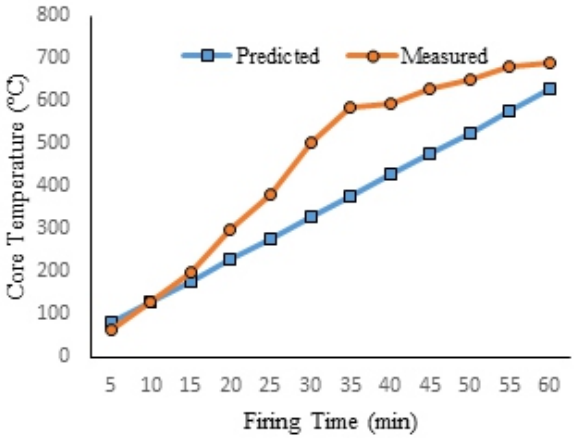

Figure 6q: Model Validation of Fuel combination 3:5:2

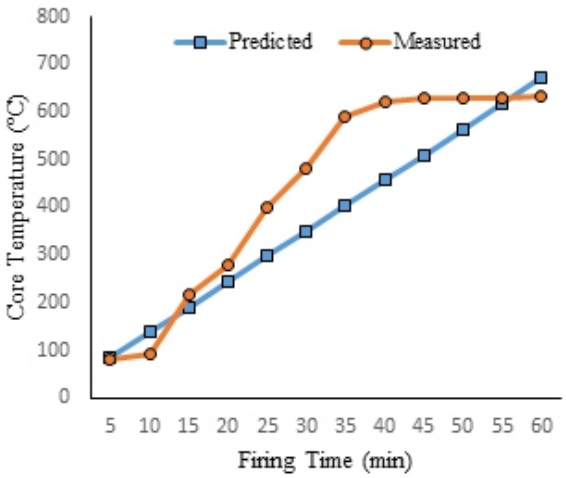

Figure 6r: Model Validation of Fuel combination 5:2:3

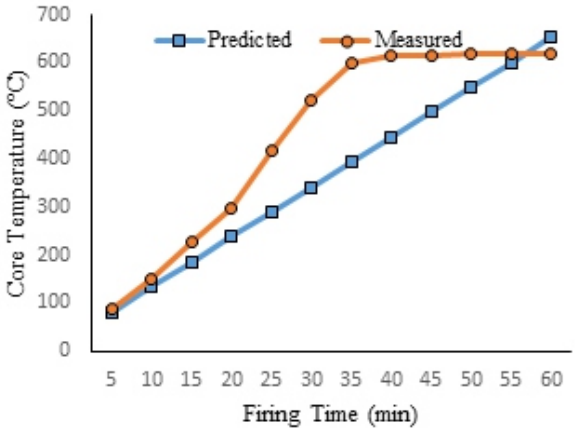

Figure 6s: Model Validation of Fuel combination 5:3:2

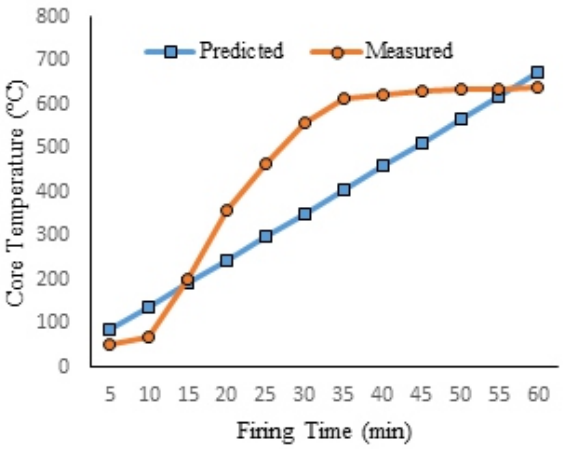

Figure 6t: Model Validation of Fuel combination 4:2:4

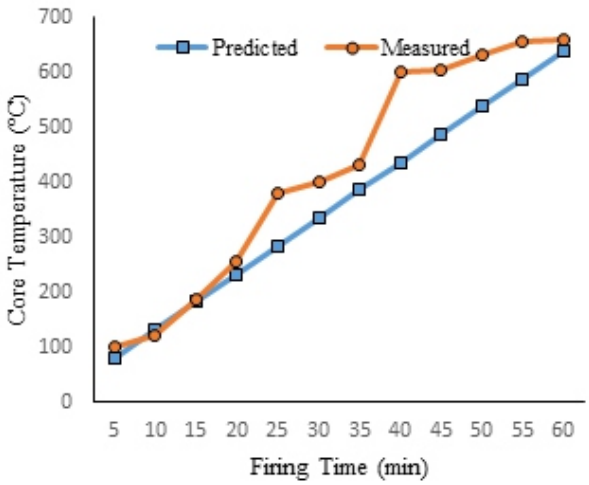

Figure 6u: Model Validation of Fuel combination 4:4:2

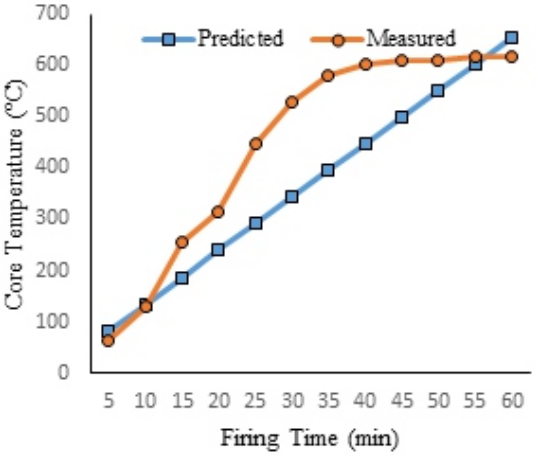

Figure 6v: Model Validation of Fuel combination 4:3:3

CONCLUSION

Conclusively, the findings from this study has provided an insight into the theoretical prediction of the boiler performance under different operating conditions and has also provided the basis for further optimization of its design and capacity scale-up.

Some of the values for predicted / experimental results for steam temperature profile include: 154 / 156 °C; 158 / 150 °C; 166 / 159 °C; 149/ 161 °C after 60 minutes firing time while some of the predicted / experimental results for furnace core temperature profile after 60 minutes firing time include: 704 / 605 °C; 678 / 611 °C; 595 / 613 °C; 650 / 640 °C; 637 / 640 °C etc. The predicted result obtained is in line with the experimental result as the result of the model validation showed that the predicted and experimental values of average steam temperature and furnace core temperature compare well with overall deviation value of about 0.12 and 1.68%.

Notations

h_w	water / steam enthalpy (kJ/kg)
$\dot{m}_w$	mass flow rate of steam or water (kg/s)
c,	specific heat capacity of the fuel (J/kg.K)
ΔT	temperature change (K)
t	time (s)
C_f	lower heating value of the biomass fuel (kJ/kg)
C_p	heat capacity at average temperature (J/K)
Cp	Specific heat capacity (J / (kg.K))
e_x	percentage excess air level (%)
h	specific enthalpy of sat. steam passing out of the shell (SH steam section) (kJ/kg)
h	specific enthalpy (kJ/kg)
$h_{ss\ out}$	specific enthalpy of sat. steam passing out of the shell (sat. steam section)
h_a	specific enthalpy of air
h_f	enthalpy of feed water (kJ/kg)
h_{fg}	specific enthalpy of furnace gas
h_s	specific enthalpy of steam
h_w	enthalpy of feedwater
k	thermal conductivity in W/m.K
$\dot{m}_{s\ in}$	mass flow rate of steam into the shell (sat. steam section) (kg/s)
$\dot{m}_{ss\ in}$	mass flow rate of steam into the shell (SH steam section) (kg/s)
m,	mass of the fuel sample (kg)
$\dot{m}_a$	mass flow rate of air (kg/s)
$\dot{m}_f$	mass flow rate of fuel
$\dot{m}_{fg}$	mass flow rate of furnace gas through the boiler.
$\dot{m}_{fw}$	mass flow rate of feed water
q	quantity of fuel used per hour (kg/hr).
V_{bf}	volume of the combustion chamber of the furnace (m^3)
V_{fg}	volume of the tube (water+steam section).
ε	stoichiometric air/fuel volume ratio
ϱ_{fg}	density of flue gas in the tube (water+steam section) (kg/m^3)

REFERENCES

Bai, X-S., Griselin, N., Klason, T. and Nilsson, J. 2002. CFD modelling of biomass combustion in small-scale boilers Final report. https://www.osti.gov/etdeweb/servlets/purl/20316669

Chen, C. 1977. Modelling a thermal power plant drum-type boiler for control: a parameter identification approach. unpublished PhD. Thesis of the Department of Electrical Engineering, Iowa State University, Ames, Iowa.

Collazo, J., Porteiro, J., Míguez, J.L., Granada, E. and Gómez, M. 2012. Numerical simulation of a small-scale biomass boiler. *Energy Conversion and Management*, 64, 87–96.
doi: 10.1016/j.enconman.2012.05.020

Haq, E.U., Rahman, T.U., Ahad, A., Ali, F. and Ijaz, M. 2016. Modelling and simulation of an industrial steam boiler. *International Journal of Computer Engineering and Information Technology*, 8, 7–10.

Hani, M.R., Mahidin, M., Husin, H., Khairil, K., Hamdani, H., Erdiwansyah, E., Hisbullah, H., Faisal, M., Mahyudin, M., Muhtadin, M., Afkar, M.I., Taka, O. and Mel, M. 2020. Experimental Studies on Combustion Characteristics of Oil- Palm Biomass in Fluidized-Bed: A Heat Energy Alternative. *Journal of Advanced Research in Fluid Mechanics and Thermal Sciences*, 68, 9–28.
doi: 10.37934/arfmts.68.2.928

Johnston Boiler Company (JBC) 2016. Common Boiler Formulas; Steam and Combustion Technology Inc. www.steamcombustion.com. Retrieved on 24th of October 2017

Li, J., Paul, M.C., Younger, P.L., Watson, I., Hossain M. and Welch, S. 2016. Prediction of high-temperature rapid combustion behaviour of woody biomass particles. Fuel, 165, 205–214.
doi: 10.1016/j.fuel.2015.10.061

Mahlia, T.M.I., Abdulmuin, M.Z., Alamsyah, T.M.I. and Muklishien, D. 2003. Dynamic modeling and simulation of a palm wastes boiler. Renewable Energy, 28, 1235–1256.
doi: 10.1016/S0960-1481(02)00218-5

Mižáková, J., Piteľ, J., Hošovský, A., Pavlenko, I., Ochowiak, M., Khovanskyi, S. 2021. Biomass Combustion Control in Small and Medium-Scale Boilers Based on Low Cost Sensing the Trend of Carbon Monoxide Emissions. *Processes*, 9(11), 2030.
doi: 10.3390/pr9112030

Jamshidi, M., Jahangiri, Q., Manesh, R.E., Azimi, S., Darvishi, H., & Nemati, B. 2012. Identify and Simulation a Furnace of Steam Boiler Based on a New Fuzzy Modelling Approach. *International Journal of Computer Science Issues*, 9(4), 1–8.

Najmi, W.A., Mohamed, W. and Abdullah, N.R. 2008. Combustion Characteristics of Palm Shell, and Palm Fibers Using an Inclined Grate Combustor. Faculty of Mechanical Engineering University of Technology MARA 40450 UiTM Shah Alam Malaysia.

Nazaruddin, Y.Y., Aziz, N.A. and Prijatna, O. 2008a. Improving Performance of PID Controller Using Artificial Neural Network for Disturbance Rejection of High Pressure Steam Temperature Control in Industrial Boiler, Int. Conf. on Control, Automation and Systems 2008, in COEX Seoul, Korea, 2008.

Nazaruddin, Y.Y., Aziz, N.A. and Sudibjo, W. 2008b. Improving the Performance of Industrial Boiler Using Artificial Neural Network Modeling and Advanced Combustion Control, Int. Conf. on Control, Automation and Systems 2008, Oct. 14-17, in COEX Seoul, Korea, 2008.

Oladosu, K.O., Ajayeoba, A.O., Kareem, B., Akinnuli, B.O. 2018. Development and Cost Estimation for Sizing 5 Kw Palm Kernel Shell Steam Boiler. *American Journal of Engineering Research* (AJER), 7(6), 113–122.

Salako, Y.A. 2011. Development of Small Scale Palm Fruit Biomass Fired Boiler unpublished MSc. Thesis of the Department of Agricultural Engineering, Obafemi Awolowo University, Ile-Ife.

Salako, Y.A., Owolarafe, O.K. and Anozie, A.N. 2009. Characterisation of Sun-Dried Palm Fruit Waste Biomass Materials. *Ife Journal of Technology*, 18(2), 26–30.

Salako, Y.A., Owolarafe, O.K. and Anozie, A.N. 2014. Performance evaluation of a small scale palm fruit biomass-fired boiler. Agric Eng Int: CIGR Journal, 16(4), 51–56.

Santos, M., André, J., Mendes, R. and Ribeiro, J.B. 2017. Design and modelling of a small scale biomass-fueled CHP system based on Rankine technology. *Energy Procedia*, 129, 676–683. doi: 10.1016/j.egypro.2017.09.143

Sebastian, T. (2002) Basics of Steam Generation. Energy Engineering and Environmental Protection Publications. Steam Boiler Technology eBook. Helsinki University of Technology Department of Mechanical Engineering.

Sebastian, T. and Antto, K. 2002. Boiler Calculations. Energy Engineering and Environmental Protection Publications. Steam Boiler Technology eBook. Helsinki University of Technology Department of Mechanical Engineering.

Tawfeic, S.R. 2013. Boiler Drum-Level Modelling. *Journal of Engineering Sciences*, Assuit University, Faculty of Engineering, 5, 1812–1829.

Xuan, S., Aute, V. and Radermacher, R. 2006. Generic Dynamic Model for Heat Exchangers. International Refrigeration and Air Conditioning Conference. Paper 819. http://docs.lib.purdue.edu/iracc/819